Atmos. Chem. Phys., 7, 377–396, 2007
www.atmos-chem-phys.net/7/377/2007/

Atmospheric Chemistry and Physics

Comparisons between ground-based FTIR and MIPAS N_2O and HNO_3 profiles before and after assimilation in BASCOE

C. Vigouroux[1], M. De Mazière[1], Q. Errera[1], S. Chabrillat[1], E. Mahieu[2], P. Duchatelet[2], S. Wood[3], D. Smale[3], S. Mikuteit[4], T. Blumenstock[4], F. Hase[4], and N. Jones[5]

[1]Belgian Institute for Space Aeronomy (BIRA-IASB), Brussels, Belgium
[2]Institut d'Astrophysique et de Géophysique, University of Liège (ULg), Liège, Belgium
[3]National Institute for Water and Atmospheric Research (NIWA), Lauder, Otago, New-Zealand
[4]Institute of Meteorology and Climate Research (IMK), Forschungszentrum Karlsruhe and University of Karlsruhe, Karlsruhe, Germany
[5]University of Wollongong, Wollongong, Australia

Received: 29 May 2006 – Published in Atmos. Chem. Phys. Discuss.: 1 September 2006
Revised: 7 December 2006 – Accepted: 14 January 2007 – Published: 23 January 2007

Abstract. Within the framework of the Network for Detection of Atmospheric Composition Change (NDACC), regular ground-based Fourier transform infrared (FTIR) measurements of many species are performed at several locations. Inversion schemes provide vertical profile information and characterization of the retrieved products which are therefore relevant for contributing to the validation of MIPAS profiles in the stratosphere and upper troposphere. We have focused on the species HNO_3 and N_2O at 5 NDACC-sites distributed in both hemispheres, i.e., Jungfraujoch (46.5° N) and Kiruna (68° N) for the northern hemisphere, and Wollongong (34° S), Lauder (45° S) and Arrival Heights (78° S) for the southern hemisphere. These ground-based data have been compared with MIPAS offline profiles (v4.61) for the year 2003, collocated within 1000 km around the stations, in the lower to middle stratosphere. To get around the spatial collocation problem, comparisons have also been made between the same ground-based FTIR data and the corresponding profiles resulting from the stratospheric 4D-VAR data assimilation system BASCOE constrained by MIPAS data. This paper discusses the results of the comparisons and the usefullness of using BASCOE profiles as proxies for MIPAS data. It shows good agreement between MIPAS and FTIR N_2O partial columns: the biases are below 5% for all the stations and the standard deviations are below 7% for the three mid-latitude stations, and below 10% for the high latitude ones. The comparisons with BASCOE partial columns give standard deviations below 4% for the mid-latitude stations to less than 8% for the high latitude ones. After making some corrections to take into account the known bias due to the use of different spectroscopic parameters, the comparisons of HNO_3 partial columns show biases below 3% and standard deviations below 15% for all the stations except Arrival Heights (bias of 5%, standard deviation of 21%). The results for this species, which has a larger spatial variability, highlight the necessity of defining appropriate collocation criteria and of accounting for the spread of the observed airmasses. BASCOE appears to have more deficiencies in producing proxies of MIPAS HNO_3 profiles compared to N_2O, but the obtained standard deviation of less than 10% between BASCOE and FTIR is reasonable. Similar results on profiles comparisons are also shown in the paper, in addition to partial column ones.

Correspondence to: C. Vigouroux
(Corinne.Vigouroux@bira-iasb.oma.be)

1 Introduction

MIPAS, Michelson Interferometer for Passive Atmospheric Sounding[1] (Fischer and Oelhaf, 1996; ESA, 2000), is one of the 10 instruments on board the European satellite ENVISAT which was launched into a sun-synchronous polar orbit at 800 km altitude, on March 1, 2002. This Fourier transform spectrometer operates in the mid infrared (4.15–14.6 µm or 685–2410 cm^{-1}) and measures high-resolution (0.025 cm^{-1} unapodised) radiance spectra at the Earth's limb. It provides day and night vertical profiles of a large number of atmospheric species with a complete global coverage of the Earth obtained in 3 days.

Part of the validation of the MIPAS Level 2 products is performed within the ENVISAT Stratospheric Aircraft and Balloon Campaigns (ESABC) or by comparisons with data from other limb sounding instruments such as HALOE (the

[1]http://envisat.esa.int/instruments/mipas/

Published by Copernicus GmbH on behalf of the European Geosciences Union.

HALogen Occultation Experiment on UARS, the Upper Atmosphere Research Satellite[2]). Additional independent measurements for the validation of MIPAS are perfomed by the ground-based Fourier transform infrared (FTIR) solar absorption spectrometers, like those operated in the framework of the Network for the Detection of Atmospheric Composition Change (NDACC[3], formerly called NDSC, Network for the Detection of Stratospheric Change). The implementation of the Optimal Estimation Method, described in Rodgers (2000), in the inversion schemes of the ground-based FTIR spectra allows the retrieval of low resolution vertical profile information (in addition to the standard total column amounts), and the characterization of the retrieved products. When it comes to verifying the MIPAS profiles at their full vertical resolution, the FTIR data cannot compete with the high vertical resolution measurements coming from balloon, aircraft or limb sounding satellite experiments. The particular benefit of using ground-based FTIR data lies in the fact that these measurements are performed regularly under clear-sky conditions, at many stations distributed over the globe, and thus represent a very interesting complementary data set for performing a statistically sound validation, and for monitoring the quality of the MIPAS products on the longer term. These ground-based FTIR data are therefore useful for contributing to the validation of MIPAS profiles in the stratosphere and upper troposphere.

Some preliminary results of MIPAS validation by balloon, aircraft, satellite, ground-based measurements, and data assimilation systems (including BASCOE) have been presented in the second workshop on Atmospheric Chemistry Validation of Envisat (ACVE-2) in May 2004 (ESA, 2004a) for all the MIPAS ESA Level 2 products, that are the vertical profiles of: temperature, H_2O, O_3, NO_2, CH_4, N_2O (Camy-Peyret et al., 2004), and HNO_3 (Oelhaf et al., 2004). In the present study, we focus on a more advanced validation of the MIPAS ESA products for the year 2003, for N_2O and HNO_3, a tropospheric source species and a stratospheric reservoir species respectively, for which the FTIR technique is the only available ground-based source of data during the considered period of MIPAS operations. Five NDACC stations are involved in this work: Kiruna (67.8° N, 20.4° E, altitude 420 m a.s.l.) and Jungfraujoch (46.5° N, 8.0° E, 3580 m a.s.l.) in the northern hemisphere, and Wollongong (34.4° S, 150.9° E, 30 m a.s.l.), Lauder (45.0° S, 169.7° E, 370 m a.s.l.), and Arrival Heights (77.8° S, 166.7° E, 200 m a.s.l.) in the southern hemisphere.

This paper describes in Sect. 2 the MIPAS ESA Level 2 products and, in Sect. 3, the ground-based FTIR vertical profile data, including some information concerning the retrieval strategies used at each station and the characterization of the data products. BASCOE, a 4D-VAR chemical data assimilation system, is described in Sect. 4. In the subsequent section, we explain the adopted methodology for the comparisons for which two approaches have been used. First, we have made the comparisons with the MIPAS offline profiles (v4.61) provided by ESA, taking care to define reasonable collocation criteria that give enough coincidences to obtain relevant statistics. Then, to improve the collocations without decreasing the number of coincidences, we have compared the ground-based FTIR profiles with the products of BASCOE. In the current configuration, BASCOE is constrained with MIPAS data and thus delivers atmospheric profiles that can be considered to be proxies of the MIPAS profiles, at any location and any time. In the last part (Sect. 6), we show the results obtained from the comparisons for both molecules, N_2O and HNO_3, at the different stations, and try to answer the following two questions: (1) can we quantify the agreement between the MIPAS and the ground-based FTIR data, and (2), what are the benefits of using the results of a data assimilation system as proxies of MIPAS profiles instead of the MIPAS profiles themselves?

2 MIPAS data

The MIPAS Level 2 products are described in the MIPAS Product Handbook[4] and in Raspollini et al. (2006). The MIPAS offline data used here were provided by the ESA v4.61 data processor (ESA, 2004b). They include the N_2O and HNO_3 volume mixing ratio (vmr) profiles as well as the atmospheric pressure and temperature vertical distributions. The vertical resolution of the delivered profiles is between 3 and 4 km and their horizontal resolution is between 300 and 500 km along track.

The individual MIPAS profiles do not cover the same altitude ranges. We observed that, for the scans used in the present study, the upper altitude limits of given MIPAS vmr profiles are quite constant for all profiles: they are around 61 km for N_2O and 43 km for HNO_3. The lower limits vary a lot between a minimum of 6 km for N_2O and 9 km for HNO_3 to greater than 20 km for worst cases. The latter variability is due to the presence of clouds: the retrievals of trace gas concentrations are limited to altitudes above the cloud top height (for clouds with high opacity in the infrared). The highest cloud heights are found, as expected, in the tropical upper troposphere (sub-visible cirrus) and in the Antarctic polar vortex (polar stratospheric clouds) (Raspollini et al., 2006). To avoid the need to extrapolate MIPAS profiles beyond the altitude limits for which retrieved vmr values are provided, while keeping a statistically relevant data set, we have restricted the considered MIPAS data set to the scans for which the lower altitude limit is smaller than or equal to 12 km for N_2O and 14 km for HNO_3. This option will allow us to consider partial column values consistently above 12 km for N_2O and above 14 km for HNO_3, without including

[2] http://haloedata.larc.nasa.gov/home/

[3] http://www.ndacc.org/

[4] http://envisat.esa.int/dataproducts/mipas

Table 1. Spectral microwindows (cm^{-1}) used for the ground-based FTIR retrievals.

	N_2O		HNO_3	
Station	Microwindow limits (cm^{-1})	Interfering species	Microwindow limits (cm^{-1})	Interfering species
Kiruna	2481.3−2482.6	CO_2, CH_4, H_2O, O_3	867.0−869.6	OCS, H_2O, CO_2, C_2H_6, CCl_2F_2
	2526.4−2528.2	CO_2, CH_4, H_2O, O_3	872.8−875.2	OCS, H_2O, CO_2, C_2H_6, CCl_2F_2
	2537.85−2538.8	CO_2, CH_4, H_2O, O_3		
	2540.1−2540.7	CO_2, CH_4, H_2O, O_3		
Jungfraujoch	2481.3−2482.6	CO_2, CH_4	868.476−870.0	OCS, H_2O
	2526.4−2528.2	CO_2, CH_4, HDO		
	2537.85−2538.8	CH_4		
	2540.1−2540.7	none		
Wollongong	2481.2−2483.5	CO_2, CH_4	868.47−870.0	OCS, H_2O, NH_3, CO_2
			872.8 − 874.0	OCS, H_2O, NH_3, CO_2
Lauder & Arrival Heights	2481.2−2483.5	CO_2, CH_4	868.3−869.6	OCS, H_2O, NH_3
			872.8 − 874.0	OCS, H_2O, NH_3

extrapolated values. However, some scans can have one or two missing values that are replaced by interpolated values in the profiles.

Because of possible uncertainties in the referencing of the MIPAS profiles versus altitude (Raspollini et al., 2006), we have adopted a vertical pressure grid for making the comparisons. Daily pressure data from each station have been used to convert the FTIR altitude grid (that covers the altitude range from the local surface altitude to about 100 km) to a unique pressure grid. The MIPAS retrieved profiles were interpolated onto the same pressure grid.

3 Ground-based FTIR data

3.1 Retrieval algorithms

Vertical profile informations can be obtained from high-resolution FTIR solar occultation spectra thanks to the pressure broadening of the absorption lines which leads to an altitude dependence of the lineshapes. Two different algorithms have been used in the present work, SFIT2 and PROFFIT9. Both codes are based on a semi-empirical implementation of the Optimal Estimation Method developed by Rodgers (2000) and provide the retrieval of molecular vertical profiles by fitting one or more narrow spectral intervals (microwindows). The SFIT2 algorithm has been described in previous works (Pougatchev and Rinsland, 1995; Pougatchev et al., 1995; Rinsland et al., 1998). It was used for the spectral inversion of the FTIR data at all stations except Kiruna. The profiles of this latter station have been retrieved using the PROFFIT9 algorithm (Hase, 2000). It has been shown recently (Hase et al., 2004) that the retrieved profiles and total column amounts obtained by these two different algorithms under identical conditions are in excellent agreement (within 1% for total column amounts of N_2O and HNO_3).

In both codes SFIT2 and PROFFIT9, the retrieved state vector contains the retrieved volume mixing ratios of the target gas defined in discrete layers in the atmosphere, as well as the retrieved interfering species column amounts, and fitted values for some model parameters. These can include the baseline slope and instrumental lineshape parameters such as an effective apodization. For the stations Jungfraujoch, Wollongong, Lauder and Arrival Heights, the atmosphere is divided in 29 layers, whereas for Kiruna it is divided in 44 layers. The 29 layers have a width of 2 km below 50 km, becoming progressively larger towards the top of the atmosphere, defined here as 100 km. The widths of the 44 layers of Kiruna progressively grow from 0.4 km at the ground to 2.3 km around 50 km altitude.

3.2 Retrieval parameters

The characteristics of the FTIR retrieval results are determined by the selection of microwindows, a priori informations, as well as additional model parameters and retrieval parameter settings. The purpose of this work is not to compare the FTIR results among them, but to show whether there is an agreement between MIPAS and independent FTIR data at different locations. Except for a common choice of the a priori profiles of the two target gases (see Sect. 3.2.2 hereafter), the FTIR retrievals have been made independently at each contributing station, with retrieval parameter settings chosen such as to optimise the retrieval results. What is important in the further comparisons is that we take into ac-

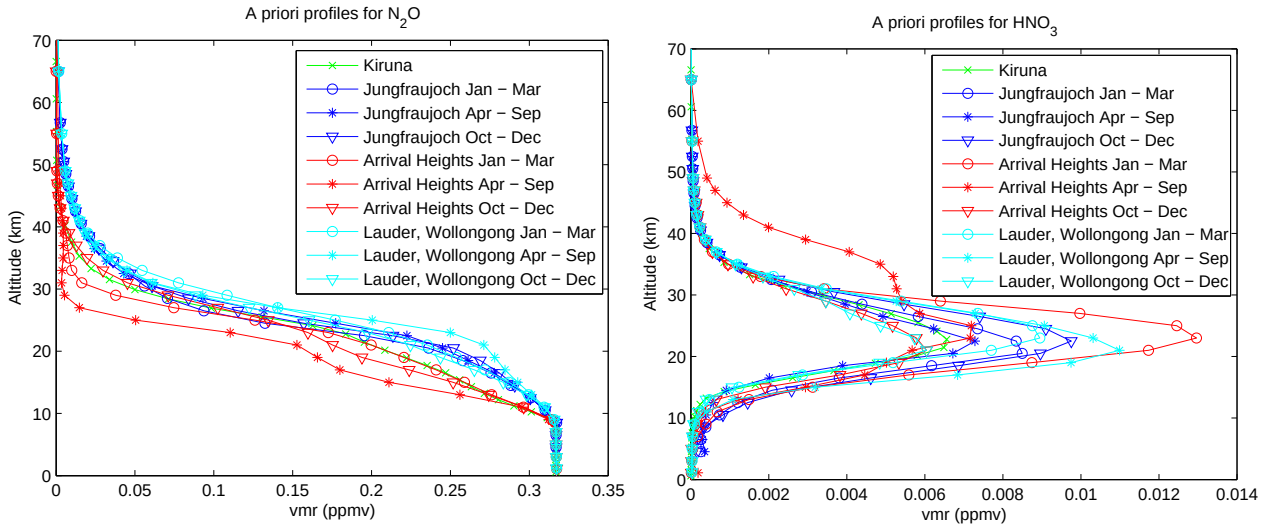

Fig. 1. N_2O and HNO_3 a priori profiles at all stations.

count the individual characteristics of the retrieval results, expressed in the averaging kernels and associated degrees of freedom for signal (DOFS), as discussed further in Sect. 3.3. Also, it is useful to know which spectroscopic data have been used in the FTIR retrievals, to have a better insight in possible biases associated herewith.

3.2.1 Spectroscopic data and spectral windows

All stations are using the spectroscopic line parameters from the HITRAN 2000 database including official updates through 2001 (Rothman, 2003). Wollongong added official updates up to August 2002 and additional lines from the Spectroscopic Atlas of Atmospheric Microwindows in the Middle Infra-Red (2nd edition) (Meier et al., 2004) but these do not include changes in the parameters for N_2O or HNO_3, or for the six interfering species, given in Table 1, that are fitted in Wollongong retrievals.

At all stations daily temperature and pressure profiles have been taken from the National Centers for Environmental Prediction (NCEP).

The retrieval microwindows used at the various stations are listed in Table 1, together with the corresponding interfering species. The a priori profiles of these interfering species are scaled simultaneously with the profile inversion of the target gases in the spectral fit procedure. Depending on location and altitude of the site and on spectral characteristics, the impact on the retrievals of fitting additional interfering species can be more or less significant. This explains why we do not always find the same interferers in the same microwindows.

3.2.2 A priori profile information

Because the inversion problem is ill-posed, the Optimal Estimation Method needs some a priori information about the retrieval state vector parameters, including the a priori vertical vmr profile $\boldsymbol{x}_a$, and the associated a priori covariance matrix $\mathbf{S}_a$ (Rodgers, 2000).

In Fig. 1, we show the a priori N_2O and HNO_3 vertical profiles used at each station. For the stations Jungfraujoch, Lauder, Arrival Heights and Wollongong, the a priori profiles have been taken identical to the climatological initial guess profiles from MIPAS for the corresponding seasons and latitude bands (so-called IG2 profiles in the MIPAS Product Handbook). Three different seasonal profiles are used, representative of the periods January to March, April to September and October to December.

For the Kiruna station, only one a priori profile is used for each species, namely the MIPAS IG2 profile for the April to September season corresponding to the latitude of Kiruna. For HNO_3 at Kiruna, the MIPAS IG2 profile has been modified below 30 km because it was found more realistic to enhance the a priori amount of HNO_3 near the tropopause.

As explained above, we do not give individual retrieval parameters such as the $\mathbf{S}_a$ matrices: we prefer to give the characterization of the retrieval results because that is the information that is used in the comparisons.

3.3 Characterization of the retrievals

As discussed in Rodgers (2000), the Optimal Estimation Method allows the characterization of the retrievals, i.e., the vertical resolution of the retrieval, its sensitivity to the a priori information and the DOFS. This is obtained by considering that the retrieved state vector $\boldsymbol{x}_r$ is related to the true state

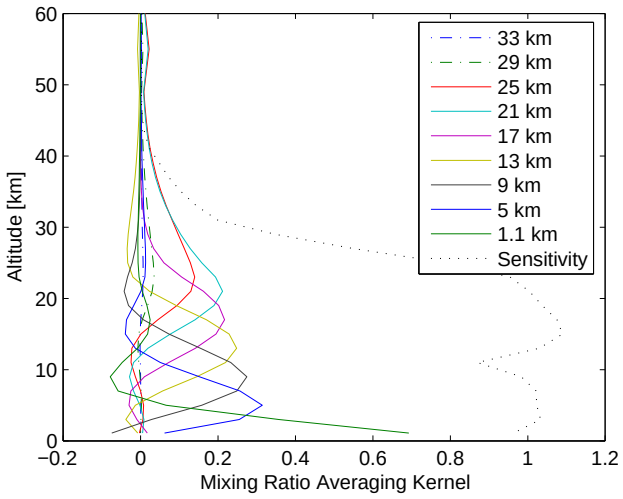

Fig. 2. Characterization of the retrieval of N_2O at Arrival Heights. Full and dashed lines: Volume mixing ratio averaging kernels (ppmv/ppmv) for the altitudes listed in the legend. Dotted line: Sensitivity of the retrieval as a function of altitude.

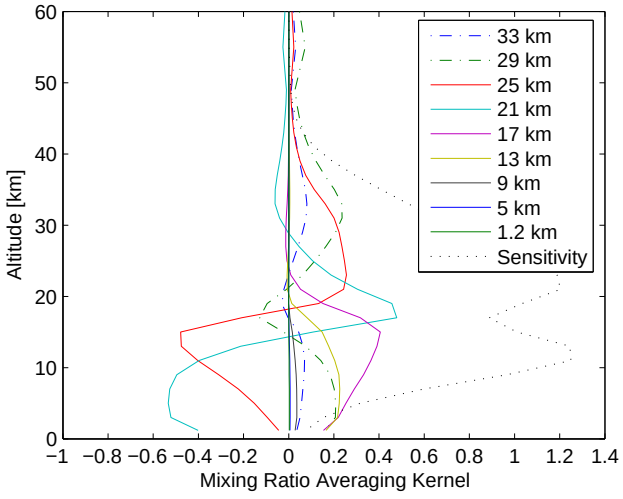

Fig. 3. Characterization of the retrieval of HNO_3 at Lauder. Full and dashed lines: Volume mixing ratio averaging kernels (ppmv/ppmv) for the altitudes listed in the legend. Dotted line: Sensitivity of the retrieval as a function of altitude.

vector $\boldsymbol{x}$ by:

$$\boldsymbol{x}_r = \boldsymbol{x}_a + \mathbf{A}(\boldsymbol{x} - \boldsymbol{x}_a) + \quad \text{error terms},$$

with $\boldsymbol{x}_a$ the a priori state vector and $\mathbf{A}$ the matrix whose rows are called the averaging kernels. The retrieved parameters are weighted means of the true and a priori state vector parameters. The weight associated with the true state vector parameters is given by the averaging kernels matrix $\mathbf{A}$ which would be the identity matrix in an ideal case where the retrieval would reproduce the truth. The actual averaging kernels matrix depends on several parameters including the solar zenith angle, the spectral resolution and signal to noise ratio, the choice of retrieval spectral microwindows, and the a priori covariance matrix $\mathbf{S}_a$. The elements of the averaging kernel for a given altitude give the sensitivity of the retrieved profile at that altitude to the real profile at each altitude, and its full width at half maximum is a measure of the vertical resolution of the retrieval at that altitude. Figures 2 and 3 show the mean averaging kernels for N_2O at Arrival Heights and for HNO_3 at Lauder, respectively. We see that the best vertical resolution is approximately 8 km for N_2O and 10 km for HNO_3.

The DOFS of the ground-based retrievals are given by the trace of the averaging kernel matrix $\mathbf{A}$. Thus, they depend on the parameters given previously, which can be different for each station and each spectrum. We have calculated, for each station, their mean value for the data used in this study. We list them for both molecules in Table 2. For HNO_3 they vary from 1.9 at the Jungfraujoch station to 2.8 at Lauder. For N_2O they vary from 4.3 at the Jungfraujoch to 3.5 at Wollongong. The high value for DOFS for N_2O at the Jungfraujoch is related to the high altitude of the station, that has a strong impact for tropospheric species.

On top of the kernels plotted in Figs. 2 and 3, we have added the so-called "sensitivity" of the retrievals at each altitude to the measurements. This sensitivity at altitude k is calculated as the sum of the elements of the corresponding averaging kernel, $\sum_i A_{ki}$. It indicates, at each altitude, the fraction of the retrieval that comes from the measurement rather than from the a priori information. A value larger than one means that the retrieved profile at that altitude is oversensitive to changes in the real profile. It may be compensating for poor sensitivity to the true profile at other altitudes when the averaging kernels do not allow the separation of the altitude ranges correctly. A value close to zero at a certain altitude indicates that the retrieved profile at that altitude is nearly independent of the real profile and is therefore approaching the a priori profile. In other words, the measurements have not significantly contributed to the retrieved profile at that altitude.

Figure 2 shows that the ground-based FTIR measurements of N_2O at Arrival Heights have a sensitivity larger than 0.5 from the ground to about 30 km altitude. For the HNO_3 retrievals at Lauder, the measurements have the largest sensitivity between 10 and 35 km, as shown in Fig. 3. The altitude range with better sensitivity does not only depend on the species considered, but it is also different at the various stations in agreement with the different values for DOFS given in Table 2. For making relevant comparisons between the ground-based and satellite data, we focus on the altitude ranges in which the sensitivity of the retrieved profiles to the measurements is sufficiently high. As we intend to compare partial column amounts, we have adopted a strict criterion to

Table 2. Characterization of the retrieved profiles of N_2O and HNO_3 at each station: statistical mean and standard deviation (1σ) for one year of measurements of the Degrees of Freedom for Signal (DOFS), and Sensitivity Range (S.R.) of the ground-based FTIR retrievals (Gd: ground; TC: total column; PC: partial column). See Sect. 3.3 for definitions.

	N_2O				HNO_3			
Station	TC DOFS	S.R. (km)	PC limits (hPa)	PC DOFS	TC DOFS	S.R. (km)	PC limits (hPa)	PC DOFS
Kiruna	3.6±0.2	Gd–25	182–24	1.3±0.2	2.5±0.5	13–36	132–4	2.0±0.3
Jungfraujoch	4.3±0.2	Gd–45	198–1	2.7±0.1	1.9±0.4	10–27	145–15	1.5±0.3
Wollongong	3.5±0.2	Gd–30	207–12	1.7±0.1	2.1±0.4	14–32	151–9	1.7±0.2
Lauder	3.7±0.3	Gd–30	199–12	1.8±0.1	2.8±0.3	8–34	144–7	2.4±0.2
Arrival Heights	3.7±0.2	Gd–28	181–17	1.5±0.1	2.8±0.4	8–34	135–7	2.2±0.2

define the altitude boundaries of these partial columns: the sensitivity, as defined above, must be larger than 0.5, which means that the retrieved profile information comes for more than 50% from the measurement, or, in other words, that the a priori information influences the retrieval for less than 50%. We have added in Table 2 these vertical sensitivity ranges (S.R.) for each molecule at each station.

It is interesting to consider the DOFS for the partial columns that will be compared between MIPAS and the FTIR data. Table 2 includes the altitude limits of these partial columns, in pressure units. The lower (in altitude) limits correspond to the lower limit of the MIPAS data of approximately 12 and 14 km for N_2O and HNO_3, respectively. The upper limits agree with the upper limit defined by the FTIR sensitivity at each station. The DOFS for the partial columns within these limits are also given in Table 2. We note that almost all of the information concerning HNO_3 from the ground-based FTIR is located within the defined partial column limits. On the contrary, for N_2O, at least half of the information is situated in the troposphere. This can also be seen in Fig. 4 where we plot three partial columns averaging kernels for both molecules: one for the partial column used in the comparisons, the two other for the partial columns in the altitude ranges above and below the considered one. The averaging kernels peak in the right altitude ranges, therefore the partial columns comparisons will not have any biases induced by the limited vertical resolution of the ground-based FTIR.

The DOFS for the partial columns are larger than one (1.3 in the worst case). Therefore, we believe that it is still valuable to show profile comparisons in Sect. 6. But, in all cases, the DOFS are lower than 2.7, thus these profile comparisons should not be over-interpreted. The detailed shapes of the profile comparisons will strongly depend on the individual FTIR averaging kernel shapes and thus on the FTIR retrieval parameters.

4 BASCOE analyses

4.1 Assimilation system and set-up

BASCOE (Belgian Assimilation System of Chemichal Observations from ENVISAT[5]) is a 4D-VAR data assimilation system derived from that described in Errera and Fonteyn (2001) (see Appendix A for a description of the similarities and the differences between both systems). BASCOE is based on a 3-D chemical transport model driven by operational ECMWF analysis (Daerden et al., 2006). MIPAS v4.61 observations of H_2O, NO_2, O_3, CH_4, N_2O, and HNO_3 have been assimilated for the year 2003. BASCOE ozone analyses have already been validated by Geer et al. (2006) who made intercomparisons of ozone analyses from different assimilation systems, including BASCOE.

The model calculates the evolution of 59 chemical species taking into account the advection, the chemistry and the Polar Stratospheric Cloud (PSC) microphysics. In the BASCOE version used here, the surface area density (SAD) of Polar Stratospheric Clouds (PSC) is parameterized in a very simple manner (see Appendix A). Heterogeneous chemistry is not parameterized, as it is solved simultaneously with gas-phase chemistry. The model extends from the surface up to 0.1 hPa using 37 levels with a horizontal resolution of 5° in longitude and 3.75° in latitude. Data assimilation is done using 4D-VAR with an assimilation window of one day. The background error standard deviation is set to 20% of the background field. Correlations are not taken into account and the background covariance matrix is therefore diagonal. Additional to the MIPAS random error, a representation error of 8.5% that takes into account the difference of resolution between BASCOE and MIPAS has been specified for each assimilated observation (Ménard et al., 2000). In order to prevent oscillating data entering into BASCOE, only values in the range [0.2, 200] hPa and [4, 200] hPa are considered for N_2O and HNO_3, respectively (M. Ridolfi, private communication).

[5]http://bascoe.oma.be/

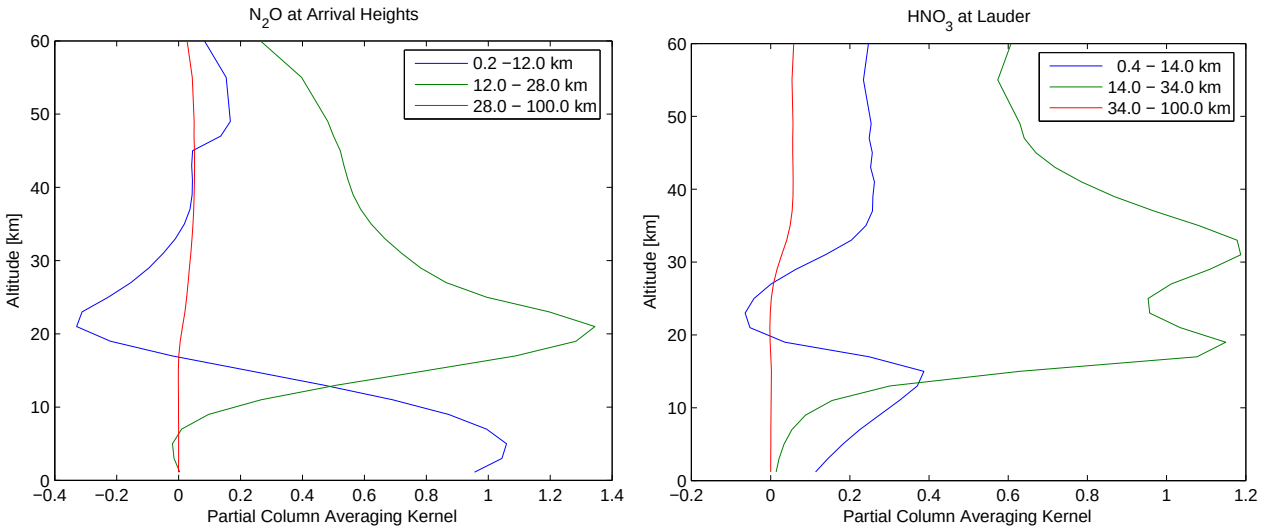

Fig. 4. Partial columns averaging kernels (mol. cm^{-2}/mol. cm^{-2}) for N_2O at Arrival Heights and HNO_3 at Lauder.

4.2 Comparison with MIPAS observations

In order to evaluate how well BASCOE represents MIPAS, we plot, in Fig. 5, the monthly mean bias (<BASCOE-MIPAS>/<MIPAS>) and standard deviation (1σ) between BASCOE and MIPAS profiles of N_2O and HNO_3 in five 10° latitude bands corresponding to each station. Generally, monthly mean N_2O biases are within ±5%. For some months, higher values are observed in the middle-high stratosphere: above 20 hPa around 75° S, above 5 hPa around 35° S and 65° N and above 3 hPa around 45° S and 45° N. However, these cases occur in pressure ranges outside the limits used to compare FTIR and MIPAS, except for the Jungfraujoch station. For the latter case, one should not take into account profiles comparison with BASCOE for pressures above 3 hPa. The effect on the comparison of partial columns of N_2O above 3 hPa is negligible, since there is almost no N_2O at high altitude (see Fig. 1). Standard deviations of monthly N_2O comparisons are between 10% to 20% within the pressure limits of the comparisons between FTIR and MIPAS, except for Arrival Heights during local winter. We also observe a significant variability from month to month. Nevertheless, this variability is comparable to the estimated assimilation error (random and representativeness errors).

For HNO_3, monthly mean biases are generally negative (BASCOE underestimates MIPAS) and vary with altitude, latitude and month. The bias is minimal, within ±5%, around 80 hPa in the −80 to −70° latitude band, and around 100 hPa in the other latitude bands. The biases are largest at 150 hPa and between 10 and 20 hPa, and vary from month to month between −10% and −30% for the worst case of Arrival Heights during local winter. Regarding the standard deviation, it is minimum around 50 hPa, the altitude at which the HNO_3 mixing ratio reaches its maximum. Within the pressure limits of the comparisons between FTIR and MIPAS, its value lies between 5% and 20% except at the South Pole where it can reach 25% in wintertime. Again, this variability is comparable to the estimated assimilation error.

4.3 Discussion

Having the above statistics in mind, we can evaluate to which extent BASCOE is a proxy of MIPAS. In the case of N_2O, we can say that BASCOE is a good proxy of MIPAS, because the bias between both is negligible. However, it is clear that BASCOE HNO_3 cannot be considered as a good absolute proxy of MIPAS because of the fact that BASCOE underestimates MIPAS HNO_3. This must be kept in mind when BASCOE will be compared to ground-based FTIR.

In order to check if the five other assimilated species could induce a bias in the HNO_3 analyses, HNO_3 has been assimilated alone for a limited period of time. No differences were found between the two sets of analyses. On the other hand, several sensitivity tests were done regarding the sulfate aerosol SAD, a quantity that is subject to large uncertainties (Küll et al., 2002). These tests result in significant changes in the agreement between MIPAS and BASCOE analyses. It is therefore expected that a different climatology of SAD than the one described in Appendix A would allow the BASCOE HNO_3 analyses to be closer to the MIPAS observations. As mentioned by Rood (2005), the problem of bias is perhaps the greatest challenge facing assimilation.

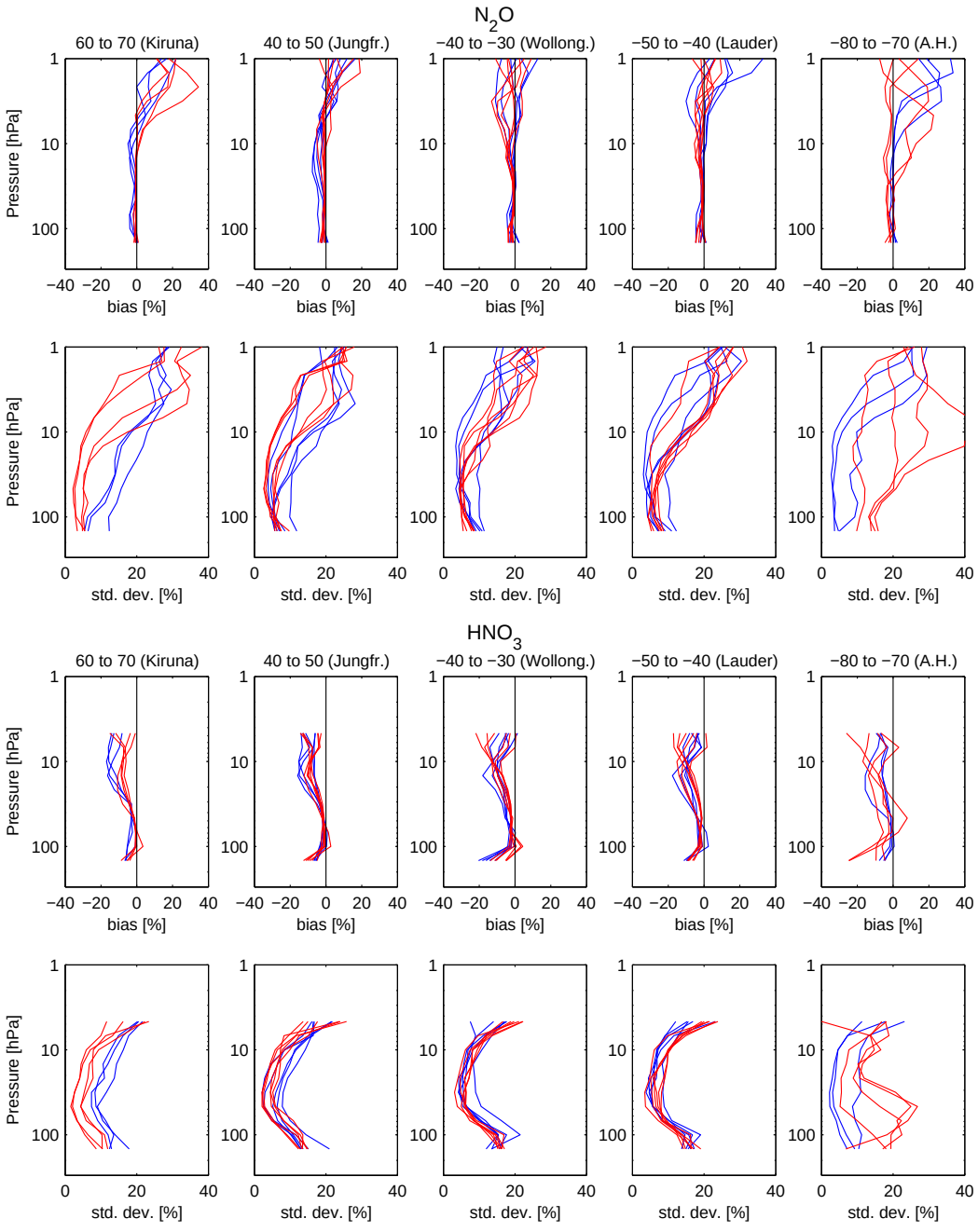

Fig. 5. Monthly zonal mean bias and standard deviation (std. dev.) between BASCOE and MIPAS profiles of N_2O (top) and HNO_3 (bottom), in 10° latitude bands around ground-based stations (A.H.: Arrival Heights). In blue: December to May; in red: June to November. For polar regions, monthly statistics are shown only for months where FTIR provides observations. Latitude are specified in °N.

5 Comparison methodologies

5.1 Vertical smoothing of the MIPAS and BASCOE profiles to the ground-based FTIR resolution

When making intercomparisons of remote sounders having different vertical resolutions, one can use the method given by Rodgers and Connor (2003) to account for that difference. In the present case, the vertical resolution of the MIPAS data is much higher than that of the ground-based FTIR data. Therefore the MIPAS profiles $\boldsymbol{x}_m$ are considered to be ideal profiles compared to ground-based FTIR ones, and the averaging kernel matrix of MIPAS retrievals is approximated

by the identity matrix. Before comparing MIPAS profiles to the ground-based ones, we smoothed them according to the characteristics of the ground-based data, following:

$$\boldsymbol{x}_s = \boldsymbol{x}_a + \mathbf{A}(\boldsymbol{x}_m - \boldsymbol{x}_a), \quad (1)$$

in which $\mathbf{x}_s$ are the smoothed MIPAS profiles and $\boldsymbol{x}_a$ and $\mathbf{A}$ are the a priori profile and the averaging kernel matrix of the ground-based FTIR retrievals, respectively. The same smoothing is applied to the BASCOE profiles.

Having adopted this approach, the vertical smoothing error (Rodgers, 2000), one of the larger FTIR error sources, which comes from the fact that the FTIR retrievals cannot see the real vertical fine structure of the atmosphere, can be neglected in the uncertainties that are to be considered in the comparison results.

It is worth noting that the smoothing procedure requires the extrapolation of MIPAS profiles beyond the altitude limits of the scan. This has been done using the MIPAS initial guess profiles.

From here onwards, we will use the terms MIPAS and BASCOE profiles for the smoothed profiles. The partial columns amounts that are discussed in the paper have been calculated from the smoothed profiles.

5.2 Statistical sets of comparisons

The four statistics defined hereinafter will be described by the mean value of the differences (the "bias") between MIPAS (or BASCOE) and FTIR and their standard deviation (1σ) (the "scatter"), in percent. To do so, we divide the mean value and the standard deviation of the absolute differences of partial columns and profiles by the mean of the FTIR partial columns and profiles, respectively. The mean value and standard deviation of our statistics are thus referring to [<MIPAS-FTIR>$\pm 1\sigma$]/<FTIR> in the tables and figures of Sect. 6. The scatter will be compared to the estimated random error on the differences to discuss the agreement between both instruments. A bias between MIPAS and FTIR will be called "statistically significant" if the mean <MIPAS-FTIR> is larger than the error on that mean, i.e., larger than $3 * \sigma/\sqrt{N}$, with N the number of coincidences.

5.2.1 Comparisons between MIPAS and ground-based profiles for two different collocation criteria

In order to obtain a statistically significant set of comparisons between the MIPAS and ground-based data, we have chosen spatial collocation circles of 1000 km radius around each of the ground-based stations. As the MIPAS tangent point can move by more than 200 km in the horizontal direction during one scan, the criterion is applied such that at least one tangent point of the scan must lie within the collocation circle. The requirement on temporal coincidence is that the recording time difference between the MIPAS and FTIR profile is smaller than 3 h. Each individual MIPAS profile is compared to the mean of the FTIR profiles that are within ± 3 h from the MIPAS measurement time. It is justified to take the mean of the ground-based measurements as the concentrations of N_2O and HNO_3 are not expected to change in such a short lapse of time. Anyway, when the standard deviation of the FTIR data set within these 6 h periods is larger than the estimated random error of the FTIR measurements, we reject that coincidence from our comparison data set. We do not take the mean of the MIPAS scans because their spatial locations and the quality of the profiles can be very different. This set of comparisons will be called "Statistics 1" in the paper.

To evaluate the impact of the collocation criterion, we will also show the results of comparisons of partial columns for a collocation of 400 km radius, with the additional requirement that all tangent points of the scan must be within the 400 km radius ("Statistics 2"). The same temporal criterion of ± 3 h is used in "Statistics 2".

The latter collocation choice leads to very poor statistics. To get around the problem of collocation, we have introduced the use of profiles obtained by the 4D-VAR data assimilation system BASCOE which can be seen as proxies of MIPAS profiles, for the species, altitude ranges and periods discussed in Sect. 4.

5.2.2 Two sets of comparisons using the 4D-VAR data assimilation system BASCOE

For the purpose of this work, BASCOE analyses have delivered vertical profiles of N_2O and HNO_3, at the location of each station, four times a day, namely at 00:00 h, 06:00 h, 12:00 h and 18:00 h UT. The comparisons between the ground-based FTIR and BASCOE data are divided in two sets. "Statistics 3" compares the means of the FTIR data sets involved in "Statistics 1", not with the collocated MIPAS profiles themselves, but with the BASCOE profiles at the location of the station that are closest in time.

To enlarge the statistics for the comparisons, we also compare the BASCOE profiles with the means of the ground-based FTIR data that are available within the six hours time ranges centered around the times of the BASCOE profiles, even if no correlative MIPAS measurements are available in these periods. This set of comparisons is referred to hereafter as "Statistics 4".

5.3 Evaluation of data uncertainties

5.3.1 Coincidence and horizontal smoothing errors

A full error analysis for comparisons between remotely sensed data sets includes not only the systematic and random uncertainties associated with each data set but also the coincidence and smoothing errors (von Clarmann, 2006). The choice of different collocation criteria and the use of BAS-

COE analyses as presented above, will allow us to estimate and to minimize the spatial coincidence error between the compared MIPAS and FTIR data sets, and to assume that the temporal coincidence error is close to zero. The vertical smoothing presented in Sect. 5.1 minimises the smoothing error in the vertical (altitude) coordinate. Additional contributions to the coincidence error come from the fact that both the MIPAS and ground-based FTIR data stem from observations that are integrated measurements along their respective line-of-sights, that may be oriented differently in space. Moreover, the sighted airmasses have a horizontal extension, that depends on the observation geometry and spectral characteristics, and that may become as large as 500 km, thus contributing to the horizontal smoothing error. These additional contributions to the coincidence and smoothing errors may become substantial if the observed target species' concentrations are non-uniform in space, over distances smaller than the sampling distances. Under these circumstances, the target species' abundances sampled by FTIR and MIPAS, and therefore also by BASCOE, may be different.

In order to further minimize the coincidence error, we have verified whether it is useful to apply an additional coincidence criteria based on the potential vorticity (PV) at the MIPAS (or BASCOE) and FTIR locations. It has turned out, however, that under circumstances where there are strong PV gradients – as is the case in local winter-spring at high latitudes -, the local PV values do not provide enough information regarding the PV gradients in the compared airmasses. In other words, we are still left with the horizontal smoothing error, which becomes substantial in these cases as well. Therefore, in such circumstances, we have decided to limit the periods for comparison to local summer-autumn periods, as will be explained further in Sect. 6.

Therefore hereinafter (Sect. 5.3.2), for the quantitative evaluation of the uncertainties associated with the comparisons, we will focus on the random uncertainties associated with both data sets. However, the residual coincidence and horizontal smoothing errors must be kept in mind when we will discuss the agreement between the data sets, in Sect. 6.

5.3.2 Random data uncertainties

We have evaluated the random error covariance matrix on the difference MIPAS-FTIR using the work of Rodgers and Connor (2003) for the intercomparison of remote sounding instruments, and of Calisesi et al. (2005) for the regridding between the MIPAS and the FTIR data. As seen before, MIPAS profiles have a much higher vertical resolution than ground-based FTIR profiles, so the random error covariance matrix of the comparison MIPAS-FTIR, $\mathbf{S}_{\delta_{12}}$ in Eq. (22) of Calisesi et al. (2005), becomes simply:

$$\mathbf{S}_{\delta_{12}} = \mathbf{S}_{x_1} + \mathbf{A}\mathbf{W}_{12}\mathbf{S}_{x_2}\mathbf{W}_{12}^T\mathbf{A}^T. \quad (2)$$

Herein $\mathbf{S}_{x_1}$ is the random error covariance matrix of the ground-based FTIR retrieved profile $\boldsymbol{x}_1$, $\mathbf{A}$ is the FTIR averaging kernel matrix specified on the FTIR retrieval grid, and $\mathbf{S}_{\boldsymbol{x}_2}$ is the random error covariance matrix of the MIPAS profile $\boldsymbol{x}_2$ specified on the MIPAS retrieval grid. $\mathbf{W}_{12}$ is a grid transformation matrix, defined by:

$$\mathbf{W}_{12} = \mathbf{W}_1^\star\mathbf{W}_2, \quad (3)$$

with $\mathbf{W}_1$ and $\mathbf{W}_2$ the transformation matrices of the FTIR and MIPAS retrieval products $\boldsymbol{x}_1$ and $\boldsymbol{x}_2$ to the equivalent retrieval products $\boldsymbol{y}_1$ and $\boldsymbol{y}_2$, respectively, on the same fine grid:

$$\begin{aligned} \boldsymbol{y}_2 &= \mathbf{W}_2\boldsymbol{x}_2 \\ \boldsymbol{x}_1 &= \mathbf{W}_1^\star\boldsymbol{y}_1. \end{aligned} \quad (4)$$

$\mathbf{W}_1^\star$ is the generalized pseudo-inverse of $\mathbf{W}_1$.

The random error matrix $\mathbf{S}_{x_1}$ for the ground-based FTIR data has been evaluated for a typical measurement at Kiruna with a solar zenith angle of 70° (F. Hase, private communication). For N_2O, the random error matrix is dominated by the contributions from the spectral baseline error, as well as the temperature profile uncertainties. For HNO_3, the spectral noise is also a dominant error source. Figure 6 shows the square-root of the variances of $\mathbf{S}_{x_1}$ for the FTIR N_2O and HNO_3 retrievals at the Kiruna station.

The ESA MIPAS products include individual error covariance matrices with each profile: they represent the errors due to the noise. As only a typical value is used for the ground-based FTIR uncertainty, we have taken for the MIPAS error covariance matrix due to noise, $\mathbf{S}_n$, the mean of the matrices corresponding to all the MIPAS scans collocated within 1000 km around the stations. A very few scans, with particularly high error values (larger than two times the mean error), have been rejected from the statistics.

An analysis of the various other sources of error of the MIPAS retrievals has been made by the Atmospheric, Oceanic and Planetary Physics (AOPP) research team at Oxford University[6]. The systematic errors given by AOPP are typical ones for large latitude bands. These errors are given in percent in an altitude grid, and it is assumed that there are no correlations between errors, i.e., each systematic error covariance matrix is diagonal. The systematic errors are divided into two parts: purely systematic errors and systematic errors with random variability. For the discussion about the scatter of the comparisons, we are interested only in the random error sources (noise and systematic errors with random variability, namely: propagation of temperature random error on the retrievals, horizontal gradient effects, uncertainties on the profiles of interfering species and on the high altitude column). Hereinafter, we will designate this random error by the short term "uncertainty". The total error covariance matrix due to all systematic error sources with random variability, $\mathbf{S}_{\text{syst\_rand}}$, has been calculated as the mean of the set of

[6]http://www.atm.ox.ac.uk/group/mipas/err/

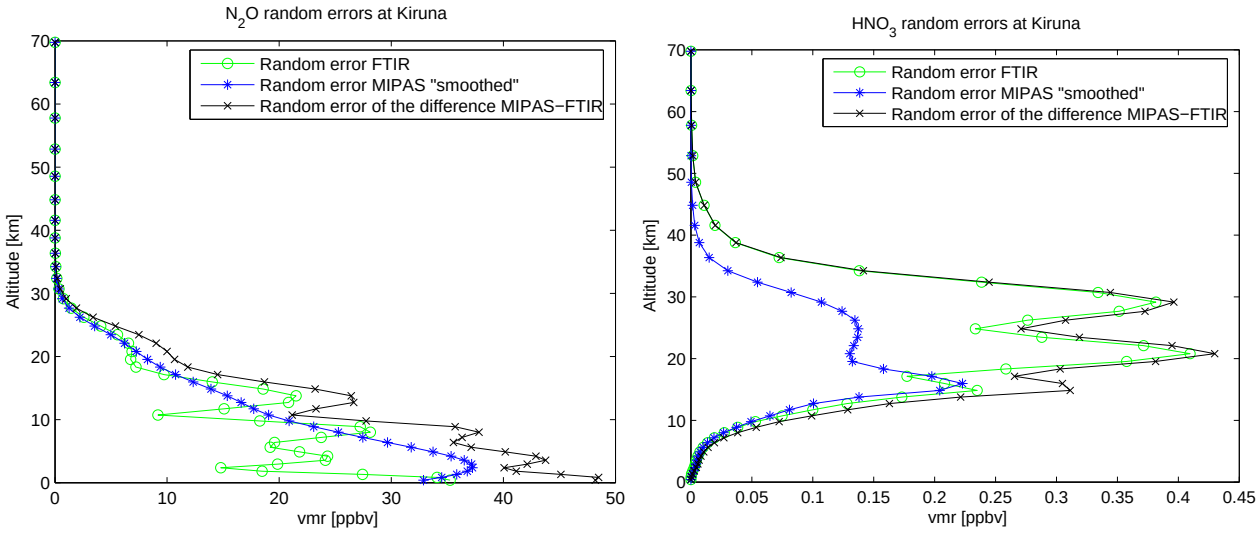

Fig. 6. Ground-based FTIR, MIPAS and (MIPAS-FTIR) random errors (in ppbv) for the N_2O and HNO_3 retrievals at Kiruna.

individual matrices in vmr units, obtained from the multiplication of the typical matrix in percentage with the individual MIPAS profile for each coincidence case.

Then the contribution of the MIPAS uncertainties to the combined random error covariance matrix $\mathbf{S}_{\delta_{12}}$ in Eq. (2) is simply: $\mathbf{S}_{x_2}=\mathbf{S}_n+\mathbf{S}_{\text{syst\_rand}}$.

Figure 6 shows the square-root of the variances of the smoothed MIPAS profile uncertainty matrix (second term on the right hand of Eq. 2) for the N_2O and HNO_3 retrievals obtained around the Kiruna station, together with the square-root of the variances of $\mathbf{S}_{x_1}$ and $\mathbf{S}_{\delta_{12}}$ for the FTIR profile and for the absolute difference MIPAS-FTIR, respectively.

From the error covariance matrix of the difference MIPAS-FTIR, we have calculated the error $\Delta_{\delta_{PC}}$ associated with the difference of partial columns. This calculation is made according to:

$$\Delta_{\delta_{PC}} = \boldsymbol{g}^T \mathbf{S}_{\delta_{12}} \boldsymbol{g}, \quad (5)$$

in which $\boldsymbol{g}$ is the operator that transforms the volume mixing ratio profile in a partial column amount, between the boundaries that have been defined earlier (Sect. 3.3 and Table 2).

Since we discuss the results of the statistical evaluations in percentage values in the next section, we calculate the relative error on the partial column differences by dividing the absolute error (Eq. 5) by the mean of the FTIR partial columns. This relative random error on the difference between MIPAS and FTIR partial columns is given in Tables 3, and 5, and will be compared to the standard deviations of the comparisons statistics to verify whether both instruments are in agreement. This is the subject of the next section.

6 Results of the intercomparisons

6.1 Results for N_2O

6.1.1 Comparisons of the partial columns of N_2O

Table 3 summarizes, for each station, the statistical results of the comparisons of the partial columns of N_2O for the four sets described in Sect. 5.2. As seen in Sect. 2, the vertical coordinate for the comparisons must be pressure rather than altitude. The pressure limits of the partial columns are repeated in the table.

Table 3 shows that there is a good agreement between MIPAS and ground-based FTIR partial columns even with the less constrained collocation criteria ("Statistics 1"). For Kiruna, Jungfraujoch and Lauder, there is no statistically significant bias between the two instruments considering the means and their error (about 2%, calculated as explained in Sect. 5.2) for "Statistics 1". A small positive bias of 4±2% is obtained at Wollongong, and a negative one of −5±2% at Arrival Heights. The random errors of the relative differences of partial columns, estimated as seen in Sect. 5.3.2, are about 6 or 7% as indicated in the table. Agreement between both instruments should give a standard deviation of the statistics similar to the estimated random errors. One expects that the remaining discrepancies of a few percent between the two instruments are due to spatial collocation criteria that are too wide. "Statistics 2", made with a reduced collocation criterion of 400 km, have indeed lower standard deviations for the three stations where the number of coincidences remains statistically relevant (≥10).

The reason why the standard deviation of the statistics is not reduced at the Kiruna station by using a stricter collo-

Table 3. Statistical means and standard deviations [<X-FTIR>$\pm 1\sigma$]/<FTIR> [%] of the N_2O partial columns confined between the given pressure limits. X stands for the MIPAS partial columns collocated within 1000 km ("Statistics 1") and 400 km ("Statistics 2") around the ground-based stations, or, the BASCOE partial columns corresponding to cases where MIPAS data exist within the adopted collocation times ("Statistics 3") and for all cases where FTIR ground-based data exist ("Statistics 4"). All X profiles have been smoothed by the ground-based FTIR averaging kernel matrices as explained in Sect. 5.1. The numbers of comparisons included in the different statistics are given between parentheses.

N_2O		[<MIPAS-FTIR>$\pm 1\sigma$]/<FTIR>					[<BASCOE-FTIR>$\pm 1\sigma$]/<FTIR>			
Station	Pressure limits [hPa]	"Statistics 1" [%]		"Statistics 2" [%]		Random error$^{\alpha}$ [%]	"Statistics 3" [%]		"Statistics 4" [%]	
Kiruna (68° N)	182–24	-1 ± 9	(283)	-4 ± 9	(6)	6	$+0\pm7$	(86)	$+0\pm7$	(119)
Jungfraujoch (46.5° N)	198–1	$+2\pm6$	(130)	$+1\pm3$	(10)	6	$+0\pm2$	(64)	$+0\pm2$	(176)
Wollongong (34° S)	207–12	$+4\pm7$	(78)	$+9\pm10$	(4)	6	$+0\pm3$	(31)	-1 ± 3	(133)
Lauder (45° S)	199–12	$+0\pm7$	(194)	$+4\pm5$	(11)	6	$+0\pm4$	(89)	$+1\pm4$	(273)
Arrival Heights (78° S)	181–17	-5 ± 10	(271)	-8 ± 9	(24)	7	-5 ± 6	(48)	-4 ± 8	(70)

$^{\alpha}$See Sect. 5.3.2 for the estimation of the error on the relative differences.

Table 4. Same as Table 3 but for a reduced (summer-autumn) time period, at Kiruna and Arrival Heights.

N_2O		[<MIPAS-FTIR>$\pm 1\sigma$]/<FTIR>					[<BASCOE-FTIR>$\pm 1\sigma$]/<FTIR>			
Station	Pressure limits [hPa]	"Statistics 1" [%]		"Statistics 2" [%]		Random error [%]	"Statistics 3" [%]		"Statistics 4" [%]	
Kiruna, June–Oct	182–24	$+1\pm5$	(187)	$+1\pm4$	(4)	6	$+0\pm3$	(54)	$+0\pm2$	(67)
Arrival Heights, Jan–March	181–17	-4 ± 5	(126)	-4 ± 4	(10)	6	-1 ± 3	(19)	-1 ± 3	(31)

cation criteria can be understood from the timeseries of the partial columns of N_2O in this particular case, as shown in Fig. 7. We see that the variation of the N_2O abundances is much higher during the winter-spring period (January to end of March), probably related to subsidence in polar vortex conditions. Thus, the higher standard deviation of 9% at Kiruna for "Statistics 1" is due to the higher variability of N_2O in time and space. This makes the collocation criterion less adequate for selecting comparable quantities. The standard deviation remains high (9%) even if the spatial collocation is set to 400 km. It is probably because in spring even a collocation of 400 km is not sufficient to take into account the N_2O spatial variability and because the horizontal smoothing error (see Sect. 5.3.1) is larger during this period. We can however not conclude because of the bad statistical conditions (only six coincidences, two of them occuring in spring). But a similar problem to Kiruna is encountered at the Arrival Heights station as seen in Fig. 8, with a high variability of N_2O in local spring (September to end of November), thus giving rise to standard deviations of "Statistics 1" and "2" (10% and 9%, respectively) that are high compared to the random error of 6%. To confirm this interpretation, the statistics of the comparisons (relative differences between FTIR and MIPAS partial column values) at Kiruna and Arrival Heights, limited to the local summer-autumn period, are given in Table 4. They show values for the standard deviations that are in agreement with the expected uncertainty for the relative differences, and that decrease from "Statistics 1" to "Statistics 2".

At the Wollongong station, "Statistics 2" suffers from a very small number of coincidences, in which essentially one out of the four MIPAS scans in coincidence, in early March, is causing the large value of the standard deviation (10%). Eliminating this point reduces the bias and the standard deviation to 4 ± 3%.

As said before, for the purpose of evaluating the impact of the collocation criteria on the comparison results, we have also compared the FTIR data with correlative data from BASCOE analyses, i.e., BASCOE analyses interpolated at the location of the ground stations as proxies for perfectly collocated MIPAS measurements, in "Statistics 3" and "4". A comparison in Table 3 of the results for "Statistics 1" to those for "Statistics 3", which include identical sets of FTIR measurements, shows lower standard deviations in the latter case, especially for the three mid-latitudes stations. A similar reduction in the standard deviations is observed in Table 4 for the two high latitude stations, Kiruna and Arrival Heights, when the reduced time period is considered. One also notices very small differences between the results (means and standard deviations) of "Statistics 3" and "Statistics 4" where BASCOE products are used even when there are no MIPAS observations that satisfy the temporal and spatial collocation

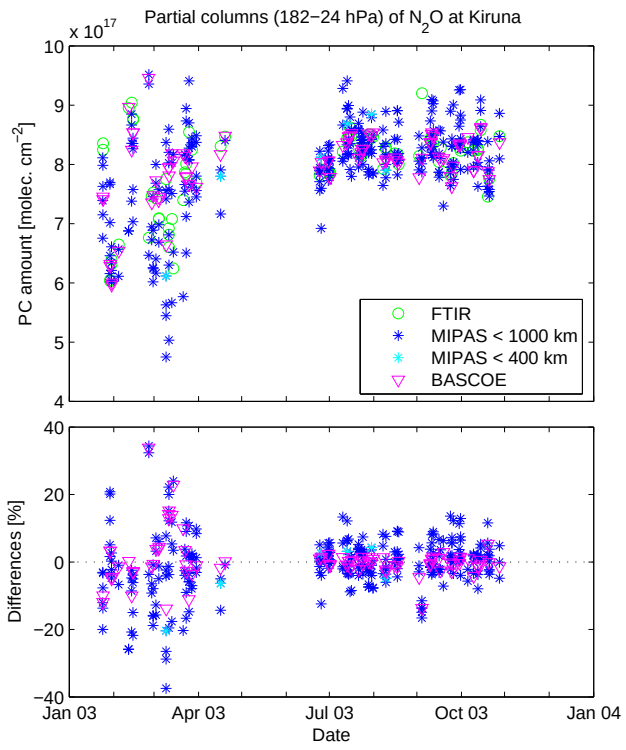

Fig. 7. Upper panel: Partial columns (182–24 hPa) of N_2O at Kiruna, from ground-based FTIR (green circles), MIPAS (dark blue and light blue stars for selections according to the spatial collocation criteria of 1000 and 400 km, respectively) and BASCOE (magenta triangles) data. Lower panel: Relative partial column differences (MIPAS-FTIR)/<FTIR> (stars; same colour coding as for upper plot), and (BASCOE-FTIR)/<FTIR> (magenta triangles).

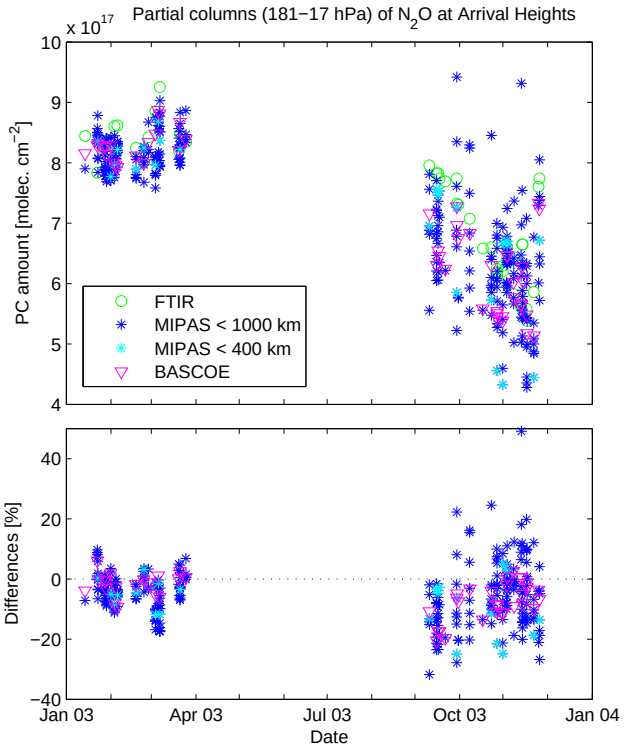

Fig. 8. Upper panel: Partial columns (181–17 hPa) of N_2O at Arrival Heights, from ground-based FTIR (green circles), MIPAS (dark blue and light blue stars for selections according to the spatial collocation criteria of 1000 and 400 km, respectively) and BASCOE (magenta triangles) data. Lower panel: Relative partial column differences (MIPAS-FTIR)/<FTIR> (stars; same colour coding as for upper plot), and (BASCOE-FTIR)/<FTIR> (magenta triangles).

criteria with the FTIR measurements. These results confirm that BASCOE products can be used reliably as proxies of MIPAS observations at any time within the considered periods. Still, in the winter-spring periods at high latitudes, where the spatial (and temporal) variability of the N_2O partial column abundances is high, it appears that BASCOE, with its resolution of 5° in longitude and 3.75° in latitude, has more difficulties to correctly capture this variability: the standard deviations of "Statistics 3" or "4" do not go down to the level of the random uncertainty (except "Statistics 3" for Arrival Heights). This is in agreement with Fig. 5 which shows that the standard deviations of the statistics comparing BASCOE and MIPAS are larger for the months January to March at Kiruna, and September to November for Arrival Heights.

One may also notice that the comparisons of BASCOE and FTIR show a significant bias only for Arrival Heights, when the whole period January to December 2003 is considered.

From the best cases (mid-latitude stations) of Table 3 and from Table 4, we see that the statistical standard deviations of the observed partial column differences can be slightly smaller than the estimated random uncertainties associated with them. This could lead to the conclusion that the uncertainty estimates for the FTIR profiles are conservative. However, we'll see in the profile comparisons in the next section that the ratio between the statistical standard deviation and the random error varies a lot with altitude (Fig. 9). The overestimation of the random error appears only in the troposphere and lower stratosphere where the amount of N_2O is important.

6.1.2 Comparisons of the vertical profiles of N_2O

Figure 9 shows the statistical means and associated standard deviations of the relative differences between the vertical profiles of N_2O from the ground-based FTIR observations and MIPAS v4.61 ("Statistics 1") and BASCOE products ("Statistics 3"), at the five contributing stations. The random error on the difference between MIPAS and FTIR profiles, i.e., the square-root of the variances of $\mathbf{S}_{\delta_{12}}$ (Eq. 2), are represented by the shaded areas around the statistical means of the MIPAS-FTIR difference profiles. As we show relative differences, the absolute errors have been divided by the mean of the FTIR profiles.

Table 5. Statistical means and standard deviations [<X-FTIR>$\pm 1\sigma$]/<FTIR> [%] of the HNO_3 partial columns confined between the given pressure limits. X stands for the MIPAS partial columns collocated within 1000 km ("Statistics 1") and 400 km ("Statistics 2") around the ground-based stations, or, the BASCOE partial columns corresponding to cases where MIPAS data exist within the adopted collocations times ("Statistics 3") and for all cases where FTIR ground-based data exist ("Statistics 4"). All X profiles have been smoothed by the ground-based FTIR averaging kernel matrices as explained in Sect. 5.1. The numbers of comparisons included in the different statistics are given between parentheses. K.: Kiruna; A.H.: Arrival Heights.

HNO_3		[<MIPAS-FTIR>$\pm 1\sigma$]/<FTIR>					[<BASCOE-FTIR>$\pm 1\sigma$]/<FTIR>			
Station	Pressure limits [hPa]	"Statistics 1" [%]		"Statistics 2" [%]		Random error [%]	"Statistics 3" [%]		"Statistics 4" [%]	
Kiruna	132–4	+12±12	(362)	+20±7	(6)	3	+5±7	(91)	+5±9	(126)
K., June-Oct		+13±9	(248)	+18±6	(4)	3	+4±6	(61)	+5±6	(74)
Jungfraujoch	145–15	+16±17	(167)	+14±12	(14)	4	+6±7	(60)	+5±8	(165)
Wollongong	151–9	+11±17	(62)	+10±3	(2)	4	+12±10	(26)	+10±9	(131)
Lauder	144–7	+15±13	(132)	+17±7	(9)	3	+4±8	(46)	+2±9	(138)
Arrival Heights	135–7	+19±23	(318)	+17±14	(33)	3	+1±13	(51)	+2±12	(68)
A. H., Jan-March		+20±9	(126)	+19±5	(10)	3	+12±4	(19)	+11±5	(28)

The black horizontal bars in Fig. 9 indicate the pressure limits of the partial columns defined in Table 3. As stated before, the MIPAS profiles are extrapolated with the MIPAS initial guess (IG2) values outside the vertical ranges of the measurements. The ground-based FTIR profiles and the smoothed MIPAS profiles tend towards the a priori profiles at altitudes where the sensitivity of the retrievals to the measurements tends to zero. This explains why the relative difference profiles and associated errors all tend to zero at high altitudes.

For Kiruna, we see in Fig. 9 a positive bias (below 3%) between MIPAS and FTIR at low altitudes becoming negative (below 5%) for pressure smaller than 100 hPa. This behaviour is similar for both whole and reduced periods. Considering the error on the mean of the differences (not plotted here, but calculated as discussed in Sect. 5), this bias is statistically significant only for pressure smaller than 80 hPa. The same kind of shape is seen at Lauder, the higher positive bias at low altitude (below 4%) being also statistically significant. At Jungfraujoch, the bias is positive (below 4%) for pressure greater than 40 hPa and become negative above (below 5%, for pressure greater than 20 hPa; below 10% above). At Wollongong, a high positive bias is observed (below 5% for pressure greater than 55 hPa with a maximum of 21% at 25 hPa). At Arrival Heights a negative significant bias is seen for the whole altitude range, below 8% and 5% for the whole and reduced period, respectively. The shape of the bias look very similar for both compared data sets, MIPAS and BASCOE. This confirms that for the purpose of the present comparison, the agreement between MIPAS and BASCOE N_2O, as seen in Fig. 5, allows the assimilated dataset to be a proxy of the satellite observations, with continuous coverage in space and time. This shows also that the biases between each dataset and the FTIR observations is probably not related to collocation issues, but rather to the shapes of the FTIR retrievals. As the DOFS for the FTIR N_2O retrievals between the considered pressure limits is between 1.3 and 2.7 (for Kiruna and Jungfraujoch, respectively; see Table 2), the detailed shape of the FTIR profiles strongly depends on the retrieval settings.

As seen with the partial columns comparisons in Table 3, the standard deviations of the relative differences are reduced when using collocated BASCOE products instead of the correlative MIPAS data. When comparing the random error and the statistical standard deviations, one should consider that the error calculation has been made using a typical case at Kiruna where the sensitivity is below 0.5 for altitudes greater than 25 km (Table 2). We observe that the statistical standard deviations are lower than the estimated random error for pressures greater than 100 hPa (around 15.5 km), in the troposphere and low stratosphere, where the N_2O amount is important.

6.2 Results for HNO_3

6.2.1 Comparisons of the partial columns of HNO_3

Analogous to the presentation for N_2O in Table 3, Table 5 gives the statistical results, at each station, for the comparisons between FTIR and MIPAS or BASCOE HNO_3 partial column values, according to the four statistical approaches described in Sect. 5.2. The partial column limits (in pressure units) are also included in the second column of Table 5.

The first striking observation is that there exists a negative bias between the FTIR and MIPAS data, of order 11 to 19%. A negative bias is expected and has been observed in previous validation work (Oelhaf et al., 2004). It is due to a scaling factor that was applied to the HNO_3 line intensities in the spectroscopic database used for the MIPAS v4.61 retrievals, mipas_pf3.1 (Flaud et al., 2003a,b; Raspollini et al., 2006), as compared to the databases used for the ground-based FTIR retrievals (HITRAN 2000, see Sect. 3.2.1). It is well-known

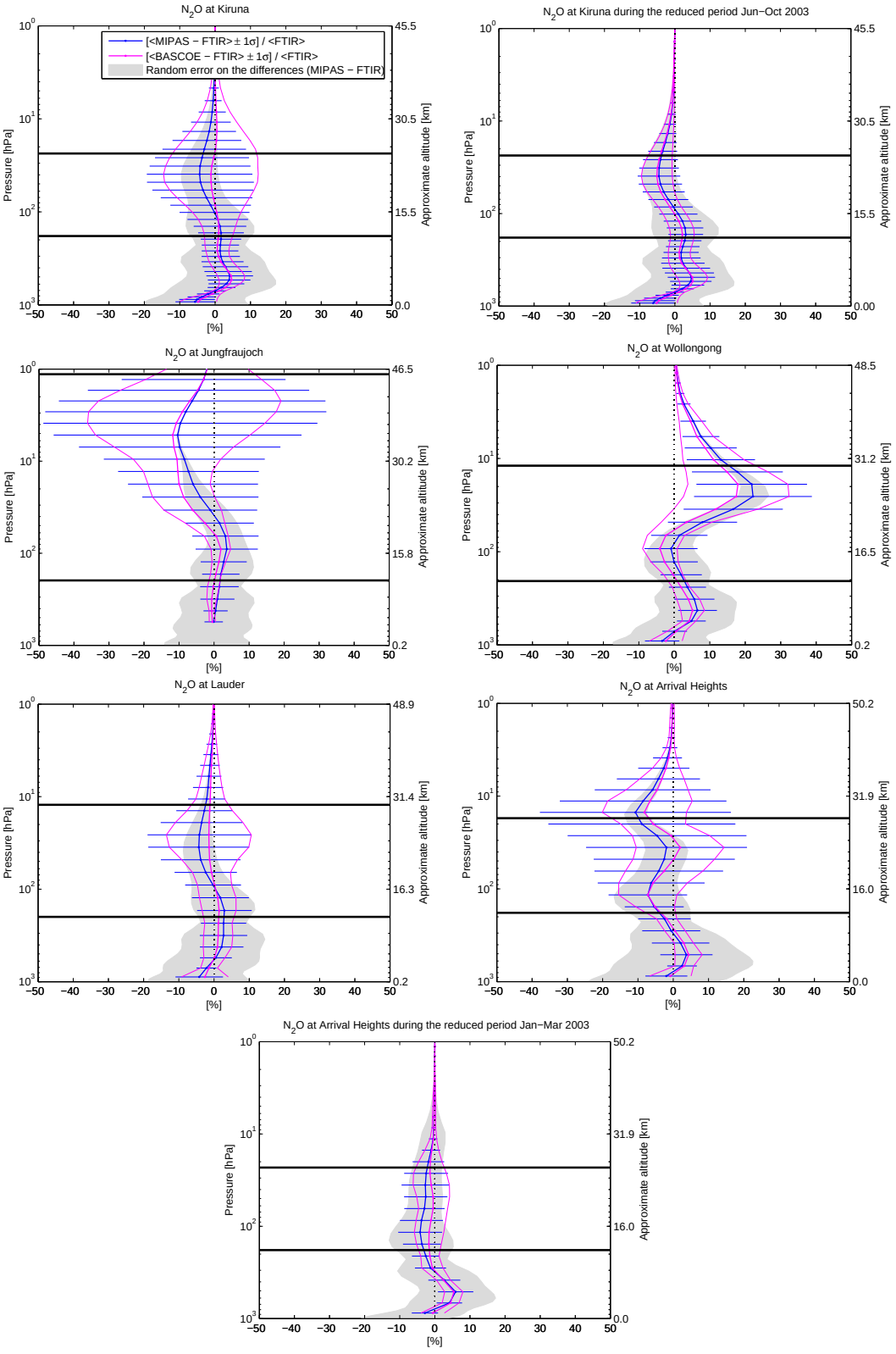

Fig. 9. Statistical means and standard deviations [<X-FTIR>$\pm 1\sigma$]/<FTIR> [%] of the N_2O difference profiles. X represents the MIPAS collocated scans within 1000 km around the stations ("Statistics 1", in blue) or the BASCOE correlative profiles ("Statistics 3", in magenta). All X profiles have been smoothed by the ground-based FTIR averaging kernel matrices as discussed in Sect. 5.1. The numbers of coincidences included in both comparison data sets are given in Table 3. The black horizontal bars indicate the pressure limits of the partial columns defined before (see also Table 3). The shaded area represents the random uncertainty on the differences, in % (see Sect. 5.3.2).

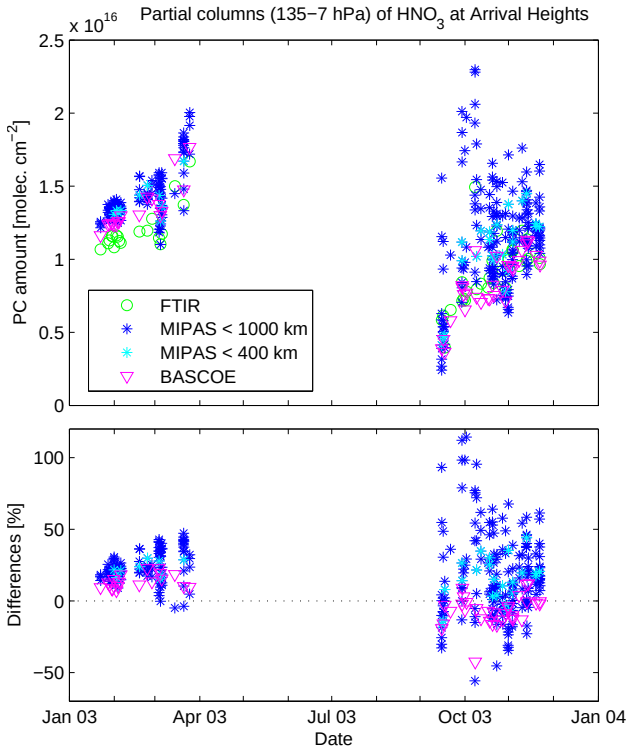

Fig. 10. Upper panel: Partial columns (135–7 hPa) of HNO_3 at Arrival Heights, from ground-based FTIR (green circles), MIPAS (dark blue and light blue stars for selections according to the spatial collocation criteria of 1000 and 400 km, respectively) and BASCOE (magenta triangles) data. Lower panel: Relative partial column differences (MIPAS-FTIR)/<FTIR> (stars; same colour coding as for upper plot), and (BASCOE-FTIR)/<FTIR> (magenta triangles).

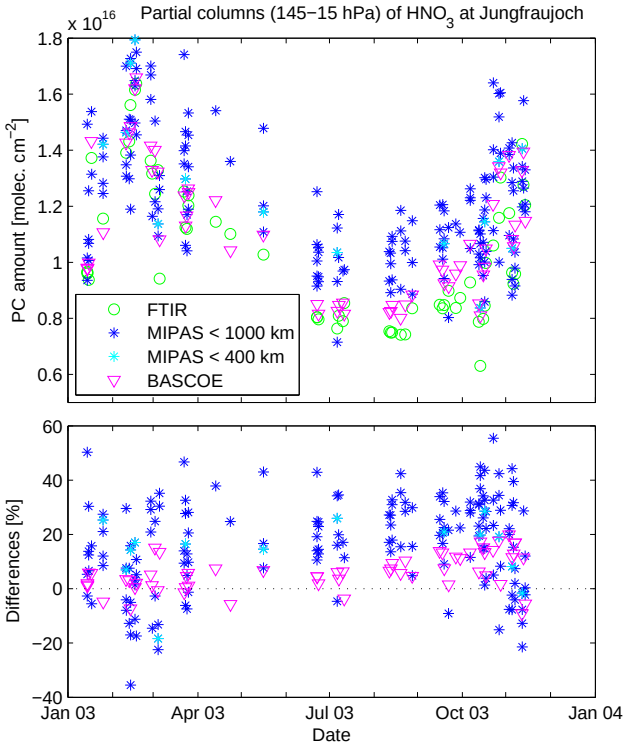

Fig. 11. Upper panel: Partial columns (145–15 hPa) of HNO_3 at the Jungfraujoch, from ground-based FTIR (green circles), MIPAS (dark blue and light blue stars for selections according to the spatial collocation criteria of 1000 and 400 km, respectively) and BASCOE (magenta triangles) data. Lower panel: Relative partial column differences (MIPAS-FTIR)/<FTIR> (stars; same colour coding as for upper plot), and (BASCOE-FTIR)/<FTIR> (magenta triangles).

that the difference in the HNO_3 spectroscopic parameters between HITRAN 2000 and mipas_pf3.1 induces a bias of about 14% between the retrieved vmr profiles (Raspollini et al., 2006). The determination of accurate HNO_3 line intensities is still controversial and in progress (see Flaud et al. (2006) and the references therein). If the same spectroscopy would have been adopted for the MIPAS and FTIR retrievals, the biases would have been 14% smaller, and thus would not have been statistically significant except for Arrival Heights. At the latter station, a mean positive bias of 5% would still be significant compared to the error on the mean of 4%.

In the case of HNO_3, the use of BASCOE analyses as proxies for the MIPAS data appears to be more problematic when one is looking at absolute concentration values. The comparisons between BASCOE and FTIR do not show the systematic bias that is observed in the direct MIPAS-FTIR comparisons, except at Wollongong. The bias between BASCOE assimilation analyses for HNO_3 and the MIPAS HNO_3 data, discussed in Sect. 4 and shown in Fig. 5, is clearly seen in Figs. 10 and 11. Even if the products of BASCOE seem to be closer to the ground-based FTIR products, it is not possible to conclude that the MIPAS measurements of HNO_3 are too high. Still, BASCOE nicely reproduces the seasonal variation.

The second noticeable fact in Table 5 is that the standard deviations of all statistics are significantly larger than expected on the basis of the random uncertainties of the relative partial column differences which are only 3 or 4%. If the same spectroscopy had been adopted for the MIPAS and FTIR retrievals, the standard deviation would have decreased by a factor of 0.86. This would give, for "Statistics 4", a standard deviation of 4% in the best case of Arrival Heights limited to the January-March period, up to 10% in the worst case of Arrival Heights when the whole year 2003 is considered. This means that the additional coincidence and horizontal smoothing errors described in Sect. 5.3.1 are significant in the comparisons between the FTIR and MIPAS products. Indeed, the additional uncertainties can largely be explained by the spatial variability of HNO_3. It is clearly seen in Table 5 by comparing "Statistics 1" and "2", that a stricter collocation criterion reduces the standard deviations significantly. One could expect that the use of BASCOE would reduce the standard deviations to the level of the estimated random un-

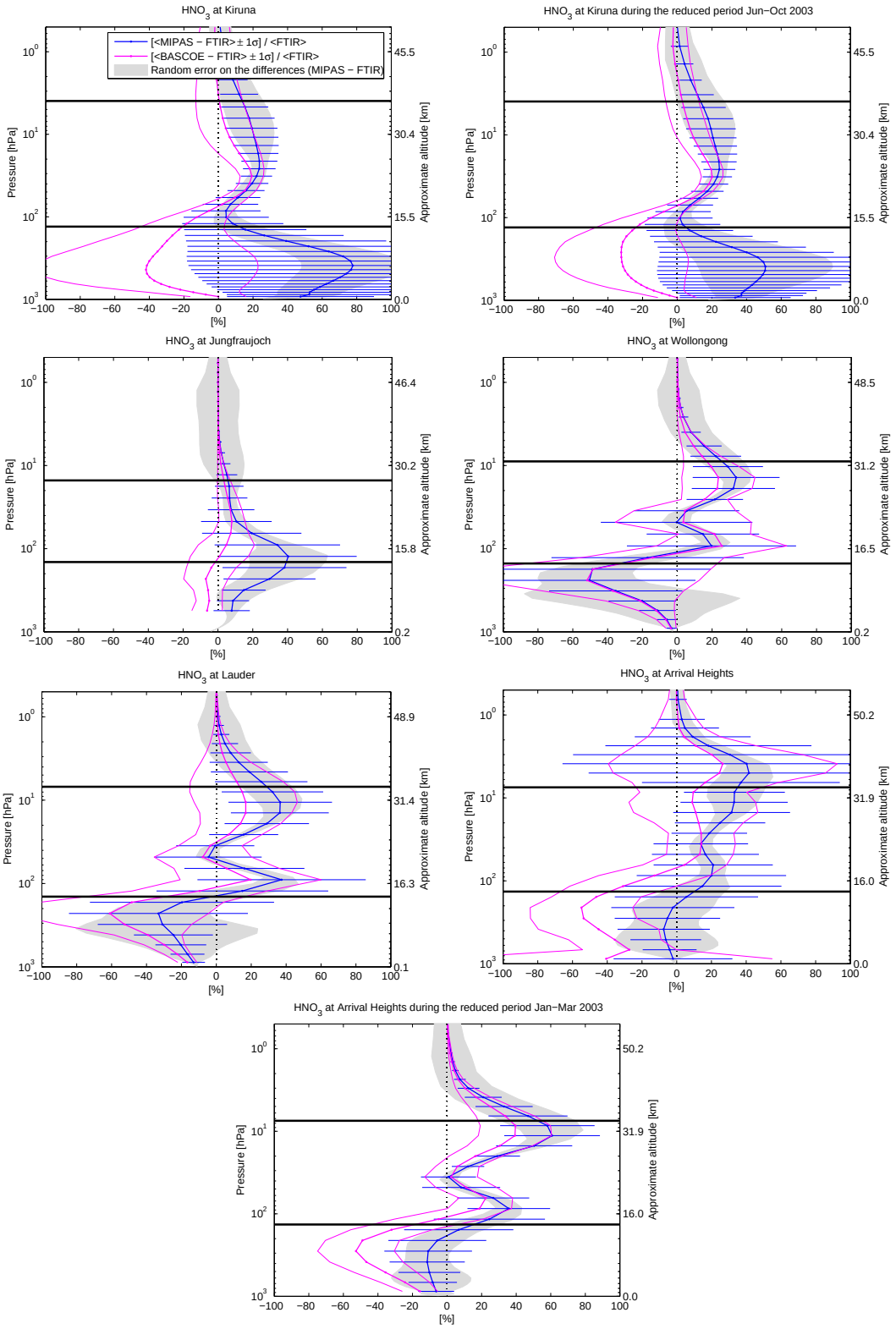

Fig. 12. Statistical means and standard deviations [<X-FTIR>$\pm 1\sigma$]/<FTIR> [%] of the HNO_3 difference profiles. X represents the MIPAS collocated scans within 1000 km around the stations ("Statistics 1", in blue) or the BASCOE correlative profiles ("Statistics 3", in magenta). All X profiles have been smoothed by the ground-based FTIR averaging kernel matrices as discussed in Sect. 5.1. The numbers of coincidences included in both comparison data sets are given in columns 1 and 3 of Table 5. The black horizontal bars indicate the pressure limits of the partial columns defined before (see also Table 5). The shaded area represents the random uncertainty on the differences, in % (see Sect. 5.3.2).

certainty, as observed for N_2O at the mid-latitude stations, but this is not the case, as shown by "Statistics 3" and "4" in the table. This means that there are additional uncertainties associated with the use of BASCOE. They could be due to inappropriate SAD for heterogeneous chemistry (see Sect. 4.3) and/or the low resolution of BASCOE (5° in longitude and 3.75° in latitude) which would not be sufficient to reproduce the HNO_3 spatial variability, as it was the case for N_2O at high latitude during the period with high variability. We see in Fig. 5 that the standard deviations of the statistics on the differences between BASCOE and MIPAS are larger during the periods of higher variability (January to March for Kiruna, and September to November for Arrival Heights). As already said, the horizontal smoothing error contributes to the observed larger standard deviations. Preliminary evaluations of this contribution indicate values that are compatible with the residual differences between the observed standard deviations and random uncertainties (C. De Clercq and J.-C. Lambert, private communication).

6.2.2 Comparisons of the vertical profiles of HNO_3

Figure 12 presents, for the five stations, the relative differences between the vertical profiles of HNO_3 for the two comparison ensembles, "Statistics 1" and "3", analogously to Fig. 9 for N_2O.

The profiles comparisons confirm the conclusions as to bias and standard deviations discussed in the previous section. First, the expected positive bias between MIPAS and FTIR, due to the use of different spectroscopy, is observed in the profiles comparisons. The shape of the bias is different from station to station: it is mainly located at 100 hPa for Jungraujoch and 30 hPa at Kiruna, whereas at Wollongong, Lauder and Arrival Heights (reduced period), the highest biases are observed at about 100 and 15 hPa. A similar shape for these three stations is not surprising as they used a similar retrieval strategy (choice of micro-windows, a priori covariance matrix,...). The DOFS for the FTIR HNO_3 retrievals between the considered pressure limits is between 1.5 (for Jungfraujoch) and 2.4 (for Lauder); therefore, the detailed shape strongly depends on the retrieval settings. Second, we can see from the different biases obtained using BASCOE compared to the MIPAS ones, that the assimilation is not as good as for N_2O, as already discussed in Sect. 4. Third, we see that the estimated random error (shaded area) is lower than the standard deviations, as obtained for the partial columns, probably due to high spatial and temporal variability of HNO_3 and the horizontal smoothing effect discussed previously. At high altitude, the relative differences go to zero but not the random uncertainty because the error calculation uses, for all the stations, a typical averaging kernel matrix of Kiruna, which has a sentivity different from zero even at high altitude.

7 Conclusions

Comparisons have been performed between MIPAS and ground-based FTIR vertical profiles of N_2O and HNO_3, covering the full year of 2003. The MIPAS data were provided by the ESA v4.61 data processor. The FTIR profiles have been retrieved at five NDACC sites distributed in latitude, namely Kiruna (68° N), Jungfraujoch (46.5° N), Wollongong (34° S), Lauder (45° S) and Arrival Heights (78° S). For the first time, the same FTIR data have also been compared with corresponding results from the 4D-VAR data assimilation system BASCOE that were obtained in the configuration in which BASCOE assimilates the ESA v4.61 products for the six primary MIPAS species (H_2O, O_3, NO_2, HNO_3, CH_4, and N_2O). This was done to evaluate the impact of the spatial collocation criteria on the comparison results and to judge the appropriateness of using BASCOE results as proxies for MIPAS profiles in the stratosphere.

Considering the comparisons between the N_2O MIPAS and FTIR lower stratosphere partial columns during the year 2003, the biases are small and significant only for Wollongong ($+4\pm2\%$) and Arrival Heights ($-5\pm2\%$). The scatter is less than 7% for the three mid-latitude stations and less than 10% for the high latitude ones. This was obtained using a coindicence criterion of 1000 km radius around the stations, and it has been demonstrated that the use of BASCOE reduces the collocation problem: the standard deviations between BASCOE and FTIR partial columns are less than 4% and 7% for the mid-latitude and high latitude stations, respectively. It has also been shown that, because the spatial resolution of the BASCOE data used here is limited to 5° longitude by 3.75° latitude, it represents less accurately the N_2O field in regions/periods with high temporal/spatial variability, such as in high latitude winter-spring conditions. Out of these periods, the standard deviation for the high latitude stations is also less than 4%, which is within the estimated random error. BASCOE profiles can indeed be considered to be good proxies for the MIPAS N_2O data.

Regarding the comparisons of HNO_3 MIPAS and FTIR partial columns, a known bias of about 14% due to the use of different spectral databases (HITRAN 2000 and mipas_pf3.1), has been confirmed. Taking this fact into account, we would not have seen any statistically significant biases except at Arrival Heights ($+5\pm4\%$). The standard deviations, corrected by the factor 0.86 for eliminating the effect of the different line-intensities, would be less than 15% at all stations except Arrival Heights where it would be 21%. These large standard deviations are partly due to the too loose coincidence criterion of 1000 km. Considering the high spatial variability of HNO_3, even with a collocation of 400 km, the statistics of the comparisons show standard deviations that are larger (by about a factor 2 to 4) than expected on the basis of the random uncertainty of the MIPAS-FTIR differences. This is explained by the fact that the HNO_3 fields exhibit variabilities on small ($<$400 km) spatial scales that can-

not be distinguished in the comparisons because the collocation is never perfect. In addition to the collocation problem, the variations of the HNO_3 field across the horizontal extension of the probed airmasses, which we call the horizontal smoothing effect, is a limitation to the agreement between both instruments. The use of BASCOE instead of MIPAS profiles cannot completely solve the collocation and smoothing problems. First, the spatial resolution of BASCOE is not sufficient. Second, at present, the horizontal smoothing effect is not taken into account appropriately. But, even then, the standard deviations of comparisons between BASCOE and FTIR are quite reasonable: after correction with the 0.86 factor, they are less than 10% for all the stations, during the whole year 2003. Concerning the biases between BASCOE and MIPAS, it turns out that in its present status, BASCOE does not provide as good proxies for the MIPAS HNO_3 profiles as for N_2O. A possible explanation of these biases is the choice of the climatology of surface area density of sulfate aerosols.

This paper has also demonstrated that ground-based FTIR measurements, despite their low vertical resolution, are usefull for satellite validation because they allow a statistical approach. They have been solicited for additional validation eforts including other independent data from balloon, aircraft and satellite.

Appendix A

This appendix describes the similarities and improvements between the 4D-VAR chemical assimilation system developped by Errera and Fonteyn (2001, hereafter denoted by EF2001) and BASCOE.

A1 Similarities

Both systems are dedicated to assimilation of stratospheric chemical observations. They used the same method (4D-VAR) and the same kind of model (3D-CTM). The adjoint of the advection scheme and the chemistry were built in the same way and both systems are minimized using a Quasi–Newton minimization method (see EF2001 for more details).

A2 Differences

The semi-lagrangian advection scheme used in EF2001 was replaced by the Flux Form Semi-Lagrangian (Lin and Rood, 1996). The number of species has been raised from 41 to 59 to include tropospheric ozone depleting tracers (CFCs, HCFCs, halons, chlorocarbons and bromocarbons). In EF2001, three categories of species are considered: (1) transported and chemically active, (2) only transported, and (3) fixed. This is no more the case. Only two species are considered fixed in BASCOE, namely N_2 and O_2. All other consituents are transported and chemically active. The chemical equation system of BASCOE has been upgraded accordingly.

Two configurations of BASCOE are possible: one with full PSC microphysics (Daerden et al., 2006) and another one with a simple parameterization for PSC surface area density (SAD). We describe now this parameterization since the present study uses BASCOE analyses obtained by the second configuration. This parameterization defines (1) SAD of ice and NAT (nitric acid trihydrate) particles when their occurrence is possible, and (2) the loss of HNO_3 and H_2O due to sedimentation. Ice PSCs are supposed to exist in the winter/spring polar regions at any grid point where the temperature is colder than 186 K, and NAT PSCs at any grid point where the temperature is colder than 194 K. The SAD is set to 10^{-6} cm^2/cm^3 in the first case and 10^{-7} cm^2/cm^3 in the second case. Finally, the SAD of the sulphate aerosols are based on a climatology by Hitchman et al. (1994). Early tests using the full PSC microphysics have shown that dividing this climatology by a factor 5 was producing better results. This factor has been kept in the present work.

Acknowledgements. The authors thank the European Commission, the Belgian Federal Science Policy Offices and ESA for funding this work through the projects UFTIR (EVK-2002-00159), Prodex CINAMON (ESA contracts 15151 and 15064) and TASTE (ESA contract 18028/04/NL/AR), respectively. They also acknowledge their national authorities for supporting the observations and the many people who have participated to them. In addition, we wish to thank the Stiftungsrat of the Jungfraujoch for supporting the facilities allowing to perform long term and regular observations at that site. The authors are also grateful to M. Ridolfi (University of Bologne) and U. Cortesi (IFAC-CNR) for discussions on MIPAS errors, and J.-C. Lambert and C. De Clercq (BIRA-IASB) for discussions on the interpretations of the results. Finally, they thank G. E. Bodeker for providing the potential vorticity values at Lauder and Arrival Heights for the FTIR and collocated MIPAS measurements.

Edited by: T. Wagner

References

Calisesi Y., Soebijanta V. T., and van Oss R.: Regridding of remote soundings: Formulation and application to ozone profile comparison, J. Geophys. Res., 110, D23306, doi:10.1029/2005JD006122, 2005.

Camy-Peyret, C., Dufour, G., Payan, S., Oelhaf, H., Wetzel, G., Stiller, G., Blumenstock, T., Blom, C. E., Guld, T., Glatthor, N., Engel, A., Pirre, M., Catoire, V., Moreau, G., De Mazière, M., Vigouroux, C., Mahieu, E., Cortesi, U., and Mencaraglia, F.: Validation of MIPAS N_2O profiles by stratospheric balloon, aircraft and ground based measurements, Proceedings of the Second Workshop on the Atmospheric Chemistry Validation of Envisat (ACVE-2), Frascati, 3–7 May 2004, ESA Special Publication SP-562, August 2004.

Daerden, F., Larsen, N., Chabrillat, S., Errera, Q., Bonjean, S., Fonteyn,. D., Hoppel, K., and Fromm, M.: A 3D-CTM with detailed online PSC-microphysics: analysis of the Antarctic winter 2003 by comparison with satellite observations, Atmos. Chem.

Phys. Discuss., 6, 8511–8552, 2006, http://www.atmos-chem-phys-discuss.net/6/8511/2006/.

Errera, Q. and Fonteyn, D.: Four-dimensional variational chemical assimilation of CRISTA stratospheric measurements, J. Geophys. Res., 106, 12 253–12 265, 2001.

ESA: Envisat-MIPAS, An instrument for Atmospheric Chemistry and Climate Research, SP-1229, published by ESA Publications Division, ESTEC, P.O. Box 299, 2200 AG Noordwijk, The Netherlands, March 2000.

ESA: Proceedings of the Second Workshop on the Atmospheric Chemistry Validation of Envisat (ACVE-2), Frascati, 3–7 May 2004, ESA Special Publication SP-562, 2004a.

ESA: Envisat-MIPAS Monthly report: March 2004, Technical Note, ENVI-SPPA-EOPG-TN-04-0011, 2004b.

Fischer, H. and Oelhaf, H.: Remote sensing of vertical profiles of atmospheric trace constituents with MIPAS limb-emission spectrometers, Appl. Opt., 35, 2787–2796, 1996.

Flaud, J. M., Piccolo, C., Carli, B., Perrin, A., Coudert, L. H., Teffo, J. L., and Brown, L. R.: Molecular line parameters for the MIPAS (Michelson Interferometer for Passive Atmospheric Sounding) experiment, J. Atmos. Ocean Optics, 16, 172–182, 2003a.

Flaud, J. M., Perrin, A., Orphal, J., Kou, Q., Flaud, P.-M., Dutkiewicz, Z., and Piccolo, C.: New anaylsis of the $\nu_5+\nu_9-\nu_9$ hot band of HNO_3, J. Quant. Spectrosc. Radiat. Transfer, 77, 355–364, 2003b.

Flaud, J. M., Brizzi, G., Carlotti, M., Perrin, A., and Ridolfi, M.: MIPAS database: Validation of HNO_3 line parameters using MIPAS satellite measurements, Atmos. Chem. Phys., 6, 5037–5048, 2006, http://www.atmos-chem-phys.net/6/5037/2006/.

Geer, A. J., Lahoz, W. A., Bekki, S., Bormann, N., Errera, Q., Eskes, H. J., Fonteyn, D., Jackson, D. R., Juckes, M. N., Massart, S., Peuch, V.-H., Rharmili, S., and Segers, A.: The ASSET intercomparison of ozone analyses: method and first results, Atmos. Chem. Phys., 6, 5445–5474, 2006, http://www.atmos-chem-phys.net/6/5445/2006/.

Hase, F.: Inversion von Spurengasprofilen aus hochaufgelösten bodengebundenen FTIR-Messungen in absorption. Wissenschaftliche Berichte Forschungszentrum Karlsruhe, FZKA 6512; ISSN 0947-8620, 2000.

Hase, F., Hannigan, J. W., Coffey, M. T., Goldman, A., Höpfner, M., Jones, N. B., Rinsland, C. P., and Wood, S. W.: Intercomparison of retrieval codes used for the analysis of high-resolution, ground-based FTIR measurements, J. Quant. Spectros. Radiat. Transfer, 87, 25-52, 2004.

Hitchman, M. H., McKay, M., and Trepte, C. R.: A climatology of stratospheric aerosol, J. Geophys. Res., 99(D10), 20 689–20 700, doi:10.1029/94JD01525, 1994.

Küll, V., Riese, M., Tie, X., Wiemert, T., Eidmann, G., Offermann, D., and Brasseur, G.: NO_y partitioning and aerosol influences in the stratosphere, J. Geophys. Res., 107(D23), 8183, doi:10.1029/2001JD001246, 2002.

Lin, S. and Rood, R. B.: Multidimensional flux–form semi–Lagrangian transport schemes, Mon. Wea. Rev., 124, 2046–2070, 1996.

Meier, A., Toon, G. C., Rinsland, C. P., Goldman, A., and Hase, F.: Spectroscopic Atlas of Atmospheric Microwindows in the middle Infra-Red, IRF Technical Report 048, ISSN 0284-1738 (Institutet för Rymdfysik, Kiruna, Sweden), Appendix E, 2004.

Ménard, R., Cohn, S. E., Chang, L. P., and Lyster, P. M.: Assimilation of Stratospheric Chemical Tracer Observations Using a Kalman Filter. Part I: Formulation, Mon. Wea. Rev., 128, 2654–2671, 2000.

Oelhaf, H., Blumenstock, T., De Mazière, M., Mikuteit, S., Vigouroux, C., Wood, S., Bianchini, G., Baumann, R., Blom, C., Cortesi, U., Liu, G. Y., Schlager, H., Camy-Peyret, C., Catoire, V., Pirre, M., Strong, K., and Wetzel, G.: Validation of MIPAS-ENVISAT version 4.61 HNO_3 operational data by stratospheric balloon, aircraft and ground based measurements, Proceedings of the Second Workshop on the Atmospheric Chemistry Validation of Envisat (ACVE-2), Frascati, 3–7 May 2004, ESA Special Publication SP-562, August 2004.

Pougatchev, N. S. and Rinsland, C. P.: Spectroscopic study of the seasonal variation of carbon monoxide vertical distribution above Kitt Peak., J. Geophys. Res., 100, 1409–1416, 1995.

Pougatchev, N. S., Connor, B. J., and Rinsland, C. P.: Infrared measurements of the ozone vertical distribution above Kitt Peak, J. Geophys. Res., 100, 16 689–16 697, 1995.

Raspollini, P., Belotti, C., Burgess, A., Carli, B., Carlotti, M., Ceccherini, S., Dinelli, B. M., Dudhia, A., Flaud, J.-M., Funke, B., Höpfner, López-Puertas, M., Payne, V., Piccolo, C., Remedios, J. J., Ridolfi, M., and Spang, R.: MIPAS level 2 analysis, Atmos. Chem. Phys., 6, 5605–5630, 2006, http://www.atmos-chem-phys.net/6/5605/2006/.

Rinsland, C. P., Jones, N. B., Connor, B. J., Logan, J. A., Pougatchev, N. S., Goldman, A., Murcray, F. J., Stephen, T. M., Pine, A. S., Zander, R., Mahieu, E., and Demoulin, P.: Northern and southern hemisphere ground-based infrared spectroscopic measurements of tropospheric carbon monoxide and ethane, J. Geophys. Res., 103, 28 197–28 217, 1998.

Rodgers, C. D.: Inverse methods for atmospheric sounding: Theory and Practice, Series on Atmospheric, Oceanic and Planetary Physics, Vol. 2, World Scientific Publishing Co., Singapore, 2000.

Rodgers, C. D. and Connor, B. J.: Intercomparison of remote sounding instruments, J. Geophys. Res., 108, 4116–4129, 2003.

Rood, R. B.: Assimilation of stratospheric meteorological and constituent observations: a review, SPARC Newsletter No. 25, 31–37, 2005.

Rothman, L. S., Barbe, A., Chris Benner, D., Brown, L. R., Camy-Peyret, C., Carleer, M. R., Chance, K., Clerbaux, C., Dana, V., Devi, V. M., Fayt, A., Flaud, J.-M., Gamache, R. R., Goldman, A., Jacquemart, D., Jucks, K. W., Lafferty, W. J., Mandin, J.-Y., Massie, S. T., Nemtchinov, V., Newnham, D. A., Perrin, A., Rinsland, C. P., Schroeder, J., Smith, K. M., Smith, M. A. H., Tang, K., Toth, R. A., Vander Auwera, J., Varanasi, P., and Yoshino, K.: The HITRAN molecular spectroscopic database: Edition of 2000 including updates through 2001, J. Quant. Spectros. Radiat. Transfer, 82, 5–44, 2003.

von Clarmann, T.: Validation of remotely sensed profiles of atmospheric state variables: strategies and terminology, Atmos. Chem. Phys., 6, 4311–4320, 2006, http://www.atmos-chem-phys.net/6/4311/2006/.